International Journal of Cancer Research 1 (1-2): 29-35, 2005
ISSN 1811-9727

Measurements of the Optical Properties of Breast Tissues *in vitro* Using Mueller Matrix Polarimetry

Shamaraz Firdous, Masroor Ikram and M. Faisal
Department of Physics and Applied Mathematics,
Pakistan Institute of Engineering and Applied Sciences,
P.O. Nilore 45650, Islamabad, Pakistan

Abstract: Laser transmittion, absorption and scattering technique for photon migration in human breast tissues phantom with Mueller matrix polarimetry have been investigated in this study. Polarized laser transmittion, including depolarization of wave applied to biological tissues provide a comprehensive frame work and simple way for diagnostic and treatment of skin lesion. He-Ne Laser (λ=632.5 nm) imaging system is described for non invasive and non radioactive clinical procedure. The system generates 16 full out put Mueller matrices for characterization of tissues. This matrix along with optical images can characterize the normal and malignant tissues for diagnostic as will as treatment procedures of breast cancer. Although the *in vitro* measurements are smaller then *in vivo*, but this research work provides a base for designing quick model of polarized laser tissues culturing and imaging.

Key words: Optical imaging, birefringence, depolarization, laser scattering, breast phantom, Mueller calculus

INTRODUCTION

Human tissue is relatively transparent to visible light in the bandwidth between 600 and 1000 nm, so that light can penetrate into tissue to a depth of up to several centimeters depending on the type of tissue. This property can be used to obtain physiological information, for example to detect tumors or to measure hemodynamic changes in tissue[1]. The determination of the optical absorption and scattering properties of tissue is of great interest for the noninvasive diagnosis by light. The particular interest in this area is the transillumination of the female breast for a preventive checkup[1,2], light screening could be an alternative to conventional x-ray mammography or could yield additional diagnostic information. The transilluminating living tissues like the female breast, the measured overall spectral characteristics are determined by recording different constituents with different wavelength dependencies of the corresponding optical parameters. Particularly the major components involved are water, fat and blood, other chromospheres for instance glucose, cytochrome and melanin are less important because their signals are very weak[3,4]. Light as a medical diagnostic tool for *in vivo* and *in vitro* tissue characterization has been used widely due to its noninvasiveness and non radioactive[5,6]. Because of the important information that light reveals, optical imaging has found many applications in biological tissue measurements[7,8]. Optical imaging has been used to probe surface structures, such as the functional activation of the exposed brain regions, skin cancers and those revealed by endoscopic procedures, but it has also been used to investigate noninvasively the internal function of large organs such as the breast[9-14]. Polarimetry is powerful tools that have been applied in various disciplines. The research in advanced polarimetry for the development of biomedical diagnostic and treatment using polarization effects of the scattered light and characterization of the samples was started[15]. The scientist have shown that polarization-based imaging measurements can provide an enhancement in superficial structures to allow for subsurface imaging[16,17]. These applications of polarimetry for biomedical imaging involve the use of Mueller-Stokes calculus to mathematically depict how a biological sample affects the polarization vector of an incident light beam, determined by either backscattered or transmitted light intensities from the sample[18,19].

Optical imaging may have a major role in breast cancer research and detection, despite its low resolution, by assessing functional and molecular cancer characteristics. The unique features of the optical method,

Corresponding Author: Shamaraz Firdous, Department of Physics and Applied Mathematics,
Pakistan Institute of Engineering and Applied Sciences, P.O. Nilore 45650, Islamabad, Pakistan
E-mail: sfirdous@pieas.edu.pk

Table 1: Calculation of the 16-image Mueller matrix. The notation is as follows: the first term represents the input polarization state, while the second term represents the output polarization state. The states are defined as: H for horizontal, V for vertical, P for+45°, M for-45°, R for right circular and L for left circular

M_{11}=HH+HV+VH+VV	M_{12}=HH+HV-VH-VV	M_{13}=PH+PV-MH-MV	M_{14}=RH+RV-LH-LV
M_{21}=HH-HV+VH-VV	M_{22}=HH-HV-VH+VV	M_{23}=PH-PV-MH+MV	M_{24}= RH-RV-LH+LV
M_{31}=HP-+HM+VP-VM	M_{32}=HP-HM-VP+VM	M_{33}=PP-PM-MP+MM	M_{34}= RP-RM-LP+LM
M_{41}=HR-HL+VR-VL	M_{42}=HR-HL-VR+VL	M_{43}=PR-PL-MR+ML	M_{44}= RR-RL-LR+LL

along with its high sensitivity for detecting photons and use of nonionizing radiation, renders optical imaging a technology that could complement existing breast imaging techniques for cancer detection and characterization. The compatibility of the technology with most other radiological imaging techniques allows the creation of combined modalities for simultaneous breast examinations that yield a superior feature set. Furthermore, optical methods are economic and can acquire data continuously, hence, they may be used for real-time monitoring[20].

Background

Optical parameters of breast tissue: The attenuation of a light beam of intensity in an absorbing solution can be described by Lambert-Beer's law. The absorption coefficient u_a is directly proportional to the concentration of the absorbing particles. In contrast, in a highly scattering medium such as biological tissue, the photons travel several times the geometric thickness of the specimen. Light attenuation in a scattering medium can be described by the scattering coefficient u_s. The anisotropy factor g describes the anisotropic distribution of the angles of light scatter, i.e. the mean cosine of the scatter angle and typical values for biological tissue range between 0.9 and 1. For more detail we can study the literature contain references on the optical parameters of breast tissue *in vivo* and *in vitro*[21-24].

Mueller matrix: To specify the polarization configuration of a radiation beam, the Stokes parameters S_0,S_1,S_2,S_3 are required. The Stokes parameters are defined as follows[25]:

$$\begin{aligned} S_0 &= \langle E_{0x}{}^2 + E_{0y}{}^2 \rangle \\ S_1 &= \langle E_{0x}{}^2 - E_{0y}{}^2 \rangle \\ S_2 &= \langle 2E_{0x}E_{0y} \cos\delta \rangle \\ S_3 &= \langle 2E_{0x}E_{0y} \sin\delta \rangle \end{aligned} \quad (1)$$

where, S_0 is the total detected light intensity which corresponds to the addition of any of the orthogonal component intensities, while S_1 is the portion of the intensity that corresponds to the difference between the square of the linear horizontal and vertical polarization states, S_2 is the portion of the intensity that corresponds to the square of the difference between the linear +45° and -45° polarization states and S_3 is the portion of the intensity that corresponds to the square of the difference between the right circular and left circular polarization states. In the present study the Mueller matrix associated with the single order transmittion by turbid phantom is studied. For simplicity, we assume that nonspherical particles are randomly oriented in space. For randomly oriented particles, having a plane of symmetry, the scattered Stokes parameters are related to their incident counterparts by the phase matrix in the following form

$$[M] = \begin{bmatrix} M_{11} & M_{12} & M_{13} & M_{14} \\ M_{21} & M_{22} & M_{23} & M_{24} \\ M_{31} & M_{32} & M_{33} & M_{34} \\ M_{41} & M_{42} & M_{43} & M_{44} \end{bmatrix} \quad (2)$$

As shown in Fig. 1, we consider a collimated radiation beam illuminating a thin layer composed of particles along the z-axis direction. For simplicity, the particles concentration is assumed to be low i.e., the optical thickness for the layer is small so that the scattered energy is essentially contributed by the first-order scattering events. One method of observing the scattered Stokes parameters is use of optical detectors or CCD camera. If such an array was placed on the x, y plane, the backscattered Stokes parameters could be related to the incident Stokes parameters as follows:

$$[S_{out}] = [M]\,[S_{in}] \quad (3)$$

where, both the incident and the scattered Stokes parameters need to be specified with a fixed laboratory reference plane. Polarized light can be completely described using the 4x1 Stokes vector, as demonstrated in Eq. 1[26]. The Mueller matrix is a mathematical representation of the optical polarization properties of a given sample in which the Stokes vector of a probing light source can be combined with the Mueller matrix of the sample to determine the polarization state of the detected output beam. knowing the input light polarization state, S_{in} and the 16 Mueller matrix element of the sample, one can determined S_{out} for a given sample (Table 1). Since biomedical imaging applications include measurements in transmission and diffuse reflectance modes, we modeled and tested our system for each of these modalities and

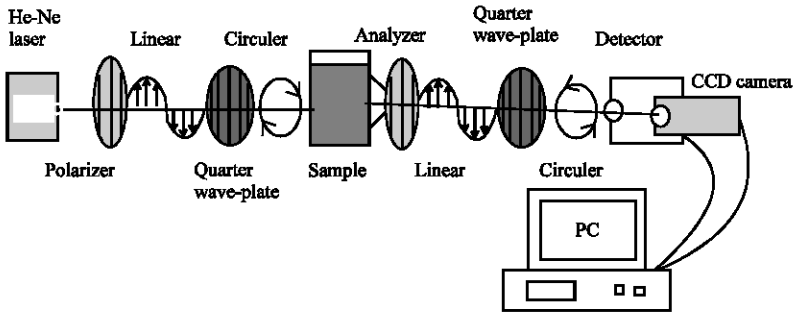

Fig. 1: Experimental setup for measurements of transmitted Mueller matrix elements. A He-Ne laser beam with an output power of 5 mW at a wavelength of 632.5 nm is used as the light source. The laser light is focused on polarizer P1 for obtaining linearly polarized light. The circularly polarized light is generated, by inserting a quarter mica retardation plate behind the linear polarizer. The out put polarized light is focus to polystyrene sphere suspension turbid medium, by lens L1 (f = 15 cm) and again pass through linear polarizer, quarter wave plate and recorded on photodiode detector and CCD camera, which is controlled and operated with Lab software

also for transmittion mode. The theory for the results we present is well developed and documented in literature[27].

MATERIALS AND METHODS

Experimental setup: The optical polarimetric imaging system, shown in Fig. 1, consists of two branches, which contain the optics necessary to create the input and output polarization states required for deriving the 16 out put Mueller matrix of breast tissue like phantom. The sample is illuminated through He-Ne laser of output power 5 mW at a wavelength of 632.5 nm. Polarization optics (dichroic sheet). is placed in front of the He-Ne laser, to generate linearly polarized light Circularly polarized light is generated, by inserting a $\lambda/4$ mica retardation plate behind the linear polarizer, with the retarder principal plane at 45^0 with respect to the electric field vector of the incident linearly polarized beam. The scattered light from the sample is focused to the analyzer and $\lambda/4$ plate for the desired variation of polarization of light. The out put light is then entered to the detector or CCD camera.

Preparation of biological tissue samples and their phantom: Freshly excised fat, liver and spleen tissues of goat were procured from a commercial butcher and cleaned thoroughly to remove dirt, if any. Thereafter, to remove traces of blood, these were soaked in physiological saline for 30 min prior to measuring their reflectance, the saline and moisture from their surfaces were mopped with blotting paper. These tissues were used within 1 h after collection. For phantom preparation of biological tissues, a hollow, conical glass model of 80 mm height and 80 mm base diameter was filled with goat fat.

RESULTS AND DISCUSSION

The measurements of media with different absorption and scattering properties (water, vegetable oil, lard, milk, Intralipid) and corresponding experimental phantom bodies (different absorbers such as balls, rods or tubes inside a highly scattering turbid medium) served as an approach to the subject (Table 2). Tissue-like media beside water and fat, the most important absorbers in all biological tissue are the blood pigments oxy-and deoxyhemoglobin (Hb and HbO). Thus all the other components play a secondary role. Figure 2 shows the transmission of these normal and malignant tissues pattern for 632.5 nm.

The main absorption feature of phantom is melanin and the strength of the fat signal or the vegetable oil in case of phanton[28] (Fig. 3). The local blood content is especially important for transillumination of living tissues because total light absorption increases with the blood concentration. This can critically limit the transmittance of thick tissues, as the absorption coefficient of whole blood increases by several orders of magnitude below 600 nm. The absorption coefficients of the individual constituents oxy (HbO) and deoxyhemoglobin (Hb) have been taken from the literature and converted into transmission data

Table 2: Absorption and scattering coefficients of normal and cancerous tissues at 632.5 nm wavelength

Tissue	Absorption coefficient (u_a)	Scattering coefficient (u_s)
Goat fat	0.63	37.2
Goat liver	1.01	14.8
Goat spleen	4.59	17.2
Normal tissue area $(cm)^3$	1.34	5.3
cancerous tissue area $(cm)^3$	0.92	7.5

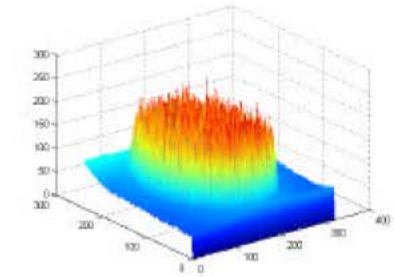

A

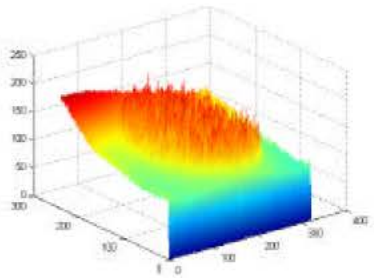

B

Fig. 2: The output transmitted intensity without polarization for (A) normal breast tissue and (B) malignant tissue

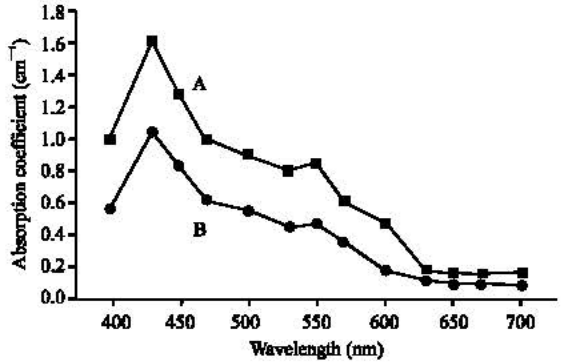

Fig. 3: Absorption spectra of breast skin tissue (A) phantom and (B) Goat tissues

to enable a comparison with the transmission characteristics of all the other contents. The mean adult hemoglobin concentration (HbO + Hb) is 2.3 mMol L^{-1} blood with an HbO fraction of around 90 to 100% in arterial blood and from 20 to 70% in venous blood sample. Thus the prime absorbers blood and water form a diagnostic window for thick biological tissue, the limit for shorter wavelengths is approximately 550 nm[28].

Measurements of highly scattering media reflect reality more closely than the merely absorbing media, i.e diluted milk and Intralipid. The results for the first medium (which consists entirely of fat) and the other two substances (which contain practically only water) clearly illustrate the spectral characteristics of these prime absorbers. In part, transmission spans three orders of magnitude (milk, Intralipid, at 40 mm thickness), the difference between water and fat characteristics between 600 and 850 nm remains small, even for highly scattering media with long path lengths[29]. There is, of course, no decrease of transmission at <600 nm because blood is completely absent. Nevertheless, such media are commonly used for phantom experiments (often mixed with absorbing dyes) since they do approximately model spectral tissue characteristics.

The experimentally measured Mueller matrix from Fig. 1 in the case of no sample is in the form of the identity matrix for each reconstruction case, as described in below matrix:

$$[M] = \begin{bmatrix} 1 & 0.874 & 0.385 & -0.101 \\ 0.678 & 0.961 & 0.850 & -0.001 \\ 0.593 & 0.368 & 0.829 & -0.004 \\ 0.233 & 0.062 & 0.002 & 0.960 \end{bmatrix} \quad (4)$$

For healthy tissues

$$[M] = \begin{bmatrix} 1 & 0.774 & 0.732 & -0.001 \\ 0.778 & 0.320 & 0.50 & -0.001 \\ 0.693 & 0.468 & 0.632 & -0.104 \\ 0.033 & 0.002 & 0.102 & 0.250 \end{bmatrix} \quad (5)$$

For malignant

$$[M] = \begin{bmatrix} 1 & 0.774 & 0.632 & -0.001 \\ 0.778 & 0.61 & 0.50 & -0.001 \\ 0.593 & 0.468 & 0.882 & -0.004 \\ 0.003 & 0.002 & 0.002 & 0.693 \end{bmatrix} \quad (6)$$

The 16 output polarization Mueller matrix can characterize and provides a fingerprint for different tissues. The elements M_{11} and M_{22}, which are the addition of the orthogonal horizontal and vertical linear polarization cases, confirms that polarization imaging can be used to eliminate pigmentation aliasing and allows the observation of the underlying tissue structure. In addition, the differences in the details of the underlying

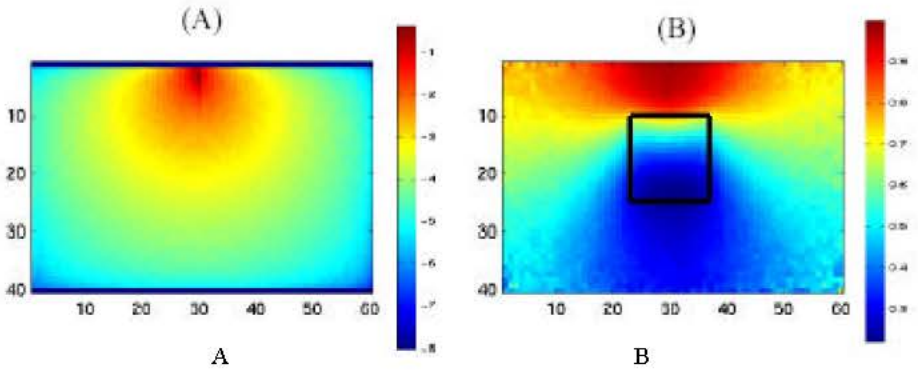

A B

Fig. 4: The transmitted output images at linearly polarized light for (A) normal and (B) cancerous tissues

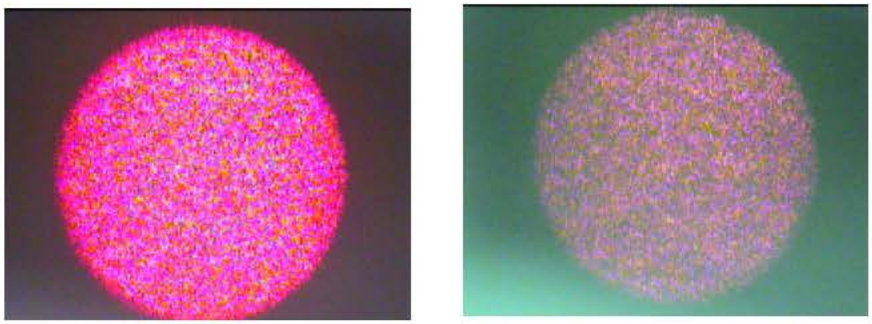

A B

Fig. 5: The transmitted output images of turbid phantom for (A) linearly polarized light and (B) circular polarized light

tissue structure between the elements other than M_{11} and M_{22}, indicate that the retention of polarization information is also dependent on the system input and output polarization states (Fig. 4). The specific experiments reported in this study have concentrated on the measurement of the scattering matrix of biological particles. One of the major problems arising in this type of experiment is related to the extreme short sampling. In addition there is deficiency in our knowledge concerning which scattering matrix elements of biological particles are of fundamental interest.

Experiments in a turbid system are mainly concerned with finite particles. Therefore, characterization of complete population is of main interest. Fortunately, symmetry conditions, especially valid for an ensemble of particles measured in a system reduce the number of independent matrix. Particles in a medium are randomly oriented on passing the laser beam. therefore ensemble averaging can be applied. the characteristics, implicit in a experiment, contribute positively to the light scattering depolarization measurements of biological particles. On the other hand, however, the complete optical equipment demands some experimental and theoretical adaptations, the sharply focused laser beam constrains the theoretical description of the interaction of a particle with the laser beam.

Furthermore a model is proposed to describe the scattering matrix of breast tissues in the medium the output Mueller matrix of air, normal and malignant tissues are given in Eq. 4-6. The difference in the linear and circular output transmittion provides detail informations about the tissues under investigation (Fig. 5). To investigate the possibility of application of a system to measure the sixteen relevant scattering matrix elements of biological particles system with exactly known scattering characteristics must be studied. It is obvious that the measurement of biological particles allows us to test the parameters of the adapted theory and the experimental setup. However, it is implicit in this test system of spheres that no major differentiation between M_{22} and M_{11} or M_{33} and M_{44} can be obtained. Therefore, the consistency of M_{22} and M_{11} was checked by additional measurement of the combinations. From these measurements M_{22} and M_{11}could be derived. No major differences in M_{11} and M_{22} were detected. Measurement of the M_{44} term was omitted since it requires a retarder analyzer. This would introduce

inevitable complications especially for the measurement of the laser signal. The consistency of M_{33} =M_{44} in the directions of the beam was verified. To explore the extent to which the 16 scattering elements can be measured, a number of independent experiments were performed. we have demonstrated that quantitative measurement of the scattering matrix elements of biological particles (Fig. 5). It has been shown that theoretical study of this type of experiment requires implementation of the beam shape into Mie scattering functions. In addition large cone integration must be applied to account for the relatively large detector surfaces.

If tissue changes (e.g. tumors) in terms of its absorption or scattering properties to differ from surrounding (healthy) tissue, it should be possible to demonstrate this as a matrix elements. Although it is difficult to simulate actual conditions in corresponding phantom experiments, we can determine the sensitivity of such experiments. For this purpose various absorbers were placed in the middle of a 40 mm thick diluted milk solution and the measured transmission spectrum was divided by the one of undiluted milk spectrum. It is logical that relative transmission values >1 indicate higher transmission by the phantom containing absorber and vice versa. The wavelength dependency of the contrast correlates depends on the difference between the absorption characteristic of the object and its surrounding media. Clinical trials will be necessary to establish the correct wavelength for detecting pathological lesions with the highest possible contrast. The tissue specimens were directly illuminated in phantom. In contrast to the tissue-like media, the blood fraction can be identified by reduced transmittance at 632.5 nm. The total transmission for the tissue thicknesses selected for these tests (20 to 30 mm) varied by more than two orders of magnitude.

CONCLUSIONS

In addition to tissue-like materials (water, vegetable oil, milk, Intralipid, lard), different types of animal tissue related to the female breast tissue *in vitro* have been investigated with the aim of correlating the dominant spectral features. Tissues that contain water are clearly distinguishable from fatty tissue on account of the absorption bands for water. The transmission differences are sufficiently clear to permit characterization of the human female breast.

The presented results establish the ability of the described Mueller matrix imaging system to precisely measure the 16 elements of a sample in either transmission and scattering modes. In the current configuration, it is clear that using 16 polarization images in the Mueller matrix reconstruction process is a trade off between maximizing accuracy a benefit of using an over determined system and acquisition time. Thus depending on the reconstruction process, it takes approximately 70 or 150 sec to reconstruct the 16 polarization images, respectively, however, it should be noted that these times are not a direct reflection of the speed of either the electro-optic components or detector. Finally, the potential of the developed system for the detection of superficial cancerous lesions lies in its ability to remove pigmentation effects and to reject deeply scattered light at different depths, based on the incident and scattered polarizations within the tissue. These effects often mask the underlying superficial structures in laser tissue imaging. In addition, the ability to fully characterize the polarization properties of the sample under investigation can provide useful information in terms of the morphological structure differences present between normal and cancerous tissue. These changes can be used to help characterize and distinguish between tissue types. Furthermore, the ability to acquire such measurements in a minimal time frame gives promise for the future application of such a system to differentiate between normal and cancerous tissue. Future studies will be directed at exploring the angular dependence of such measurements and in the development of algorithms to aid in the characterization and differentiation process.

ACKNOWLEDGMENTS

The authors acknowledge the enabling role of the Higher Education Commission Islamabad, Pakistan and appreciate its financial support through Merit Scholarship Scheme for Ph.D Studies in Science and Technology.

REFERENCES

1. Ntziachristos, V., A.H. Hielscher, A.G. Yodh and B. Chance, 2001. Diffuse optical tomography of highly heterogeneous media. IEEE. Trans. Med. Imaging, 20: 470-478.
2. Jarlman, O., I. Andersson, G. Balldin, S.A. Larsson, 1992. Diagnosticaccuracy of light-scanning mammography in women with dense breast. Acta Radiologica, 33: 69-71.
3. Jarlman, O., G. Balldin, I. Andersson, M. Lofgren, A.S. Larsson and F. Linell, 1992. Relation between light scanning and the histologic and mammographic appearance of malignant breast tumors. Acta Radiologica, 33: 63-68.

4. Hebden, J.C., H. Veenstra, H. Dehgani, E.M.C. Hillman, M. Schweiger, S.R. Arridge and D.T. Delpy, 2001. Three-dimensional time-resolved optical tomography of conical breast phantom. Applied Opt., 40: 3278-3287.
5. Muller, G.J. *et al*., 1993. Medical optical tomography: Functional imaging. SPIE IS 11, The International Society for Optical Engineering, Bellingham, Washington.
6. Chance, B. and R.R. Alfano, 1994. Quantification and localization using diffuse photons in a highly scattering medium. SPIE 2082, The International Society for Optical Engineering, Bellingham, Washington.
7. Golub, R.M., R.E. Parsons, B. Sigel, E.J. Feleppa, J. Justin, H.A. Zaren, M. Rorke and H. Kimitsuki, 1993. Differentiation of breast tumors by ultrasonic tissue characterization. Ultrasound Med., 12: 601-608.
8. Kim, E.E., D.A. Podoloff, L.A. Moulopoulos, G.N. Hortobagyi, T. Yeatman and S.E. Singletary, 1993. Magnetic resonance imaging, positron emission tomography and radio-immunoscintigraphy of breast cancer. The Cancer Bulletin, 45: 500-505.
9. Chacko, S. and M. Singh, 2000. Three-dimensional reconstruction of transillumination tomographic images of human breast phantoms by red and infrared lasers. IEEE Trans. Biomed. Eng., 47: 131-135.
10. Kienle, A., L. Lilge, M.S. Patterson, R. Hilbst, R. Steiner and B.C. Wilson, 1996. Spatially resolved absolute reflectance measurements for non-invasive determination of optical scattering and absorption coefficient of biological tissue. Applied Opt., 35: 2304-2314.
11. Welch, A.J. and V. Gemert, 1992. Optical and Thermal Response of Laser Irradiated Tissues. Plenum Press, New York, pp: 73-100.
12. Anand, N.S., D. Kumar, R. Srinivasan and M. Singh, 2003. Laser reflectance imaging of human forearms and their tissue-equivalent phantoms. Med. Biol. Eng. Comput., 41: 28-32.
13. Chacko, S. and M. Singh, 2000. Three-dimensional reconstruction of transillumination tomographic images of human breast phantoms by red and infrared lasers. IEEE Trans. Biomed. Eng., 47: 131-135.
14. Jiang, H., Y. Xu, N. Iftimia, J. Eggert, K. Klove, I. Baron and L. Fajardo, 2001. Three-dimensional optical tomographic imaging of breast in a human subject. IEEE Trans. Med. Imaging, 20: 1334-1340.
15. Srinivasan, R. and M. Singh, 2003. Laser backscattering and transillumination imaging of human tissues and their equivalent phantoms. IEEE Trans. Biomed. Eng., 50: 724-730.
16. Mujat, M. and A. Dogariu, 2001. Real-time measurement of the polarization transfer function. Applied Opt., 40: 34-44.
17. Vitkin and E. Hoskinson, 2000. Polarization studies in multiply scattering chiral media. Opt. Eng., 39: 353-362.
18. Demos, S.G. and R.R. Alfano, 1997. Optical polarization imaging. Applied Opt., 36: 150-155.
19. Cameron, B.D., M.J. Rakovic, M. Mehrubeoglu, G.W. Kattawar, S. Rastegar, L.V. Wang and G.L. Cote, 1998. Measurement and calculation of the two-dimensional backscattering Mueller matrix of a turbid medium. Opt. Lett., pp: 1630-1633.
20. Ablitt, B.P., K.I. Hopcraft, K.D. Turpin, P.C.Y. Chang, and E. Jakeman, 1999. Imaging and multiple scattering through media containing optically active particles. Waves Random Media, 9: 561-572.
21. Yao, G. and L.H. Wang, 2000. Propagation of polarized light in turbid media: Simulated animation sequences. Opt. Express, 7: 198-203.
22. Kumar, D. and M. Singh, 2003. Non-invasive imaging of optical parameters of biological tissues. Med. Biol. Eng. Comput., 41: 310-316.
23. Chacko, S., D. Kumar and M. Singh, 2003. Image reconstruction of optical attenuation coefficient variation in biological tissues. Indian J. Expt. Biol., 41: 26-32.
24. Jacques, J., 2001. Introduction to biomedical optics. Oregon Graduate Institute, http://omlc.ogi.edu/classroom/ece532.
25. Cameron, D., 2000. The application of polarized light to biomedical diagnostics and monitoring. Ph.D Thesis, Texas A and M University, College Station, TX.
26. Lianhua, J., T. Hamada, Y. Otani and N. Umeda, 2004. Measurement of characteristics of magnetic fluid by the Mueller matrix imaging polarimeter. Opt. Eng., 43: 181-185.
27. Schmitt, J.M., A.H. Gandjbakhche and R.F. Bonner, 1992. Use of polarized light to discriminate short-path photons in a multiply scattering medium. Applied Opt. 31: 6535-6546.
28. Firdous, S. M. Ikram, M. Nawaz and M. Aslam, 2004. Measurement of an optical parameters: Absorption scattering and auto-florescence of skin *in vitro*. J. Cancer Res., (In Press).
29. Srinivasan, R., D. Kumar and M. Singh, 2004. Optical characterization and imaging of biological tissues. Current Sci., 87: 218-228.